DOI: 10.1002/adma.200702088

Combinatorial Polymer Scaffold Libraries for Screening Cell–Biomaterial Interactions in 3D**

By *Yanyin Yang, Durgadas Bolikal, Matthew L. Becker, Joachim Kohn, Diana N. Zeiger,* and *Carl G. Simon, Jr.**

Dedicated to the memory of Nicola D. Richards, D.M.D., Ph.D.

We have developed a combinatorial method for screening cell–biomaterial interactions in a 3D format. Previous high-throughput approaches for screening cell–material interactions have focused on planar 2D surfaces or films. However, biomaterials are commonly used in a 3D scaffold format and cells behave more physiologically when cultured in 3D. Hence, combinatorial scaffold libraries were fabricated in 96-well plates in which polymeric, salt-leached scaffolds of varied composition and properties were present in each well. Libraries were fabricated from two biodegradable tyrosine-derived polycarbonates: poly(desaminotyrosyl-tyrosine ethyl ester carbonate) (pDTEc) and poly(desaminotyrosyl-tyrosine octyl ester carbonate) (pDTOc). During culture, osteoblast adhesion and proliferation into scaffolds were enhanced as the pDTEc content of the scaffolds increased. To our knowledge, this is the first demonstration of a method for fabricating combinatorial arrays of large-pore scaffolds (diameter (d) > 0.1 mm) for screening cell–material interactions in a 3D format.

Despite significant investments, few profitable tissue-engineering products have come to market.[1] As a result, combinatorial methods, which have accelerated pharmaceutical research,[2,3] are beginning to impact biomaterials research.[4–11] However, methods for screening cell–biomaterial interactions are mostly limited to 2D films or surfaces,[4–14] despite the facts that biomaterials are frequently used to fabricate 3D scaffolds,[15] cells exist in vivo in a 3D environment, and cells cultured in vitro in a 3D environment typically behave more physiologically than those cultured on a 2D surface.[16–20] Films and surfaces typically display a ''nanoscale'' roughness,[11,21] while processing of biomaterials into 3D scaffolds yields structures with a topographical roughness at multiple size scales. Cells are very sensitive to material topography and the large difference in structure between 2D films and 3D scaffolds should be considered when screening materials. For these reasons, a combinatorial approach in which cell–biomaterial interactions are screened using a 3D polymer-scaffold configuration will provide more relevant information regarding cell responses to test biomaterials.

We have developed a method for fabricating combinatorial libraries of polymer scaffolds where the materials are presented to cells as 3D, porous, salt-leached polymer scaffolds and many scaffold compositions can be tested in a single experiment. The libraries are designed for screening cell response so that scaffold formulations that promote or suppress cellular activity can rapidly be identified. In the current study, we have used the combinatorial approach to fabricate scaffold libraries of varying composition of two amorphous, biodegradable, biocompatible, tyrosine-derived polycarbonates: pDTEc [poly(desaminotyrosyl-tyrosine ethyl ester carbonate)] and pDTOc [poly(desaminotyrosyl-tyrosine octyl ester carbonate)].[22]

As shown in Figure 1a–b, pDTEc and pDTOc share a structurally identical backbone, but different side chains (ethyl on pDTEc and octyl on pDTOc) give the two polymers different properties. pDTEc and pDTOc have different water contact angles (71° for pDTEc and 91° for pDTOc), glass transition temperatures (99 °C for pDTEc and 53 °C for pDTOc), mechanical properties (pDTEc is brittle (4% elongation at break), while pDTOc is ductile (400% elongation at break)), and degradation rates (pDTEc degrades faster).[21,22] The respective properties affected cell response causing enhanced cell spreading, adhesion, and proliferation on films of pDTEc versus pDTOc during in vitro cell-culture experiments.[21,22] The variation of these properties also affected gene expression in osteoblast and macrophage cell lines cultured on films of the polymers and their blends.[21] These results indicate that the pDTEc/pDTOc system will elicit differences in cell behavior and will make a good test system for the combinatorial scaffold-library approach. Another reason for our interest in testing these two polymers is that tyrosine-derived polymers have successfully been used

[*] Dr. C. G. Simon Jr., Dr. Y. Yang, Dr. D. N. Zeiger, Dr. M. L. Becker
Polymers Division, National Institute of Standards and Technology
100 Bureau Drive, Gaithersburg, MD 20899-8543 (USA)
E-mail: carl.simon@nist.gov
Dr. D. Bolikal, Dr. J. Kohn
New Jersey Center for Biomaterials, Rutgers University
Piscataway, NJ 08854 (USA)

[**] We acknowledge helpful contributions from N. J. Lin, J. Sun, L. M. Pakstis, and S. Lin-Gibson (NIST). This work was supported by NIST and NIH/NIBIB R21 EB006497-01. Polymers were synthesized at Rutgers University supported by ''RESBIO'' – the Integrated Resource for Polymeric Biomaterials (NIH Grant P41 EB001046). This article, a contribution of the National Institute of Standards and Technology, is not subject to US copyright. Certain equipment and instruments or materials are identified in the paper to adequately specify the experimental details. Such identification does not imply recommendation by the National Institute of Standards and Technology, nor does it imply the materials are necessarily the best available for the purpose.

ADVANCED MATERIALS

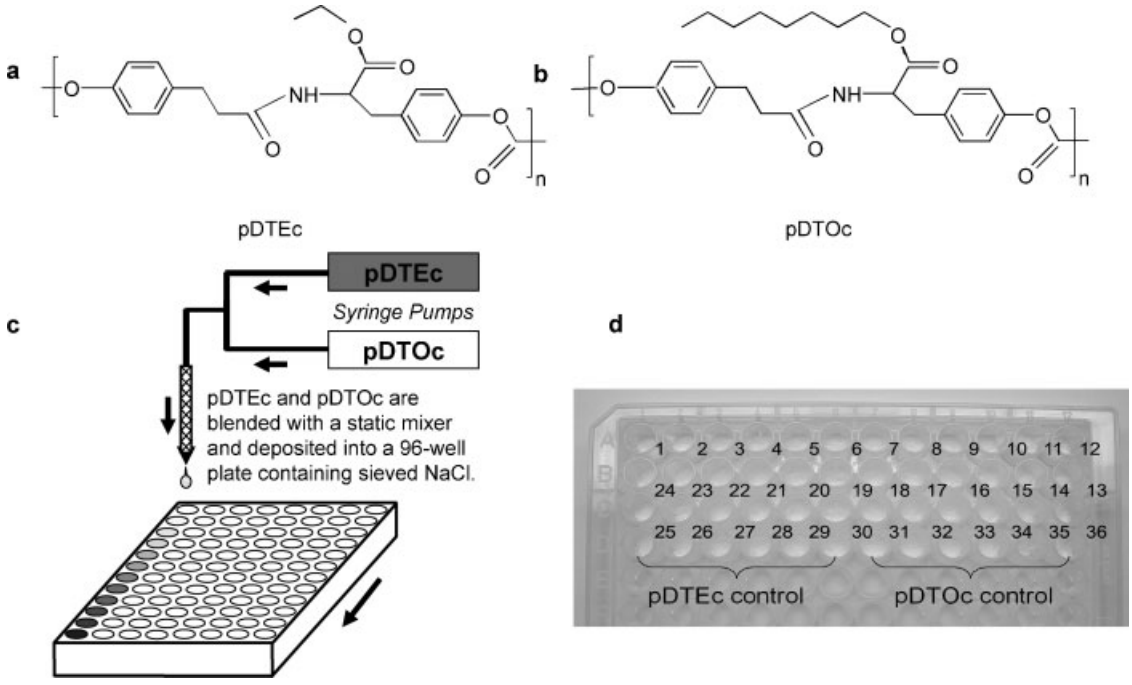

Figure 1. a) Chemical structure of pDTEc. b) Chemical structure of pDTOc. c) Illustration of combinatorial pDTEc/pDTOc scaffold library fabrication. d) An example of a freeze-dried, salt-leached scaffold library in a 96-well plate. All libraries used in this manuscript were exactly the same as the one shown. Each library had 48 scaffolds: (six pDTEc controls) + (six pDTOc controls) + (36 of varied composition).

in medical implants (hernia repair mesh and cardiovascular stents).[23]

In the current study, 3D combinatorial pDTEc/pDTOc scaffold libraries were fabricated in a 96-well plate. FTIR (Fourier transform infrared spectroscopy) and SEM (scanning electron microscopy) were used to assess library composition and structural morphology, respectively. Screening was done with the MC3T3-E1 osteoblast cell line because there is a strong need for bone substitutes and because degradable polymers are commonly used for bone tissue engineering.[15] The MC3T3-E1 cell line is a well-characterized model for osteoblasts, which follows the typical stages of osteogenesis during culture in both 2D and 3D.[15,24] Cell adhesion and proliferation were evaluated with a microplate reader assay and fluorescence microscopy. A total of 14 libraries were fabricated for this manuscript: one for SEM, one for FTIR, and 12 for cell culture. The results show that the combinatorial scaffold libraries can be used to screen for scaffold compositions that best support cell adhesion and proliferation.

Combinatorial libraries were fabricated in polypropylene 96-well plates using a two-syringe pump system (Fig. 1c) yielding arrays of salt-leached, macroporous scaffolds of varying compositions of pDTEc and pDTOc (Fig. 1d). The composition of the scaffolds in the libraries was verified using FTIR (Fig. 2a–b). The absorbance at 3000 cm^{-1}, attributed to aliphatic (CH) stretching, is stronger for pDTOc than for pDTEc; while absorbance at 1508 cm^{-1}, attributed to backbone phenyl (C=C) stretching, is the same for both polymers (Fig. 2a).[22] Hence, the ratio of peak area at 3000 cm^{-1} to the peak area at 1508 cm^{-1} can be used to determine the library composition. A calibration curve obtained from FTIR measurements of several pDTEc/pDTOc blends of known composition (Fig. 2b inset) showed a linear increase in peak ratio with increasing pDTOc content ($R = 0.98$, $p < 0.001$). The calibration curve was then used to convert the peak area ratio measurements from library scaffolds into specific compositions.[25] The results demonstrate that the composition of the libraries changes linearly from pDTEc-rich to pDTOc-rich as the well number increases ($R = 0.99$, $p < 0.001$) (Fig. 2b); these results agree with previous measurements.[26]

Large pores were observed in the scaffolds with a pore size range of 200 to 400 μm, which is suitable for bone tissue engineering (Fig. 2c–f).[27,28] Smaller voids (<10 μm) were also found in the scaffold walls (Fig. 2g–j); this may be attributed to dioxane sublimation during freeze-drying. The large (Fig. 2c–f) and small pore (Fig. 2g–j) morphology was similar for all scaffold compositions in the libraries as well as for pure pDTEc and pDTOc scaffolds (not shown) which served as controls. These results indicate that scaffold morphology was not affected by the pDTEc/pDTOc composition and suggest that any corresponding differences in cellular response can be attributed to variations in scaffold composition (not scaffold architecture). In addition, un-dissolved NaCl crystals were not found in the scaffolds indicating that all NaCl had been leached out and that the scaffold pores were interconnected.

Scaffold porosity can be calculated from the pDTEc/pDTOc density (1.2 g/cm^3), scaffold mass, and scaffold volume as described previously.[26] Total porosity is approximately 97%

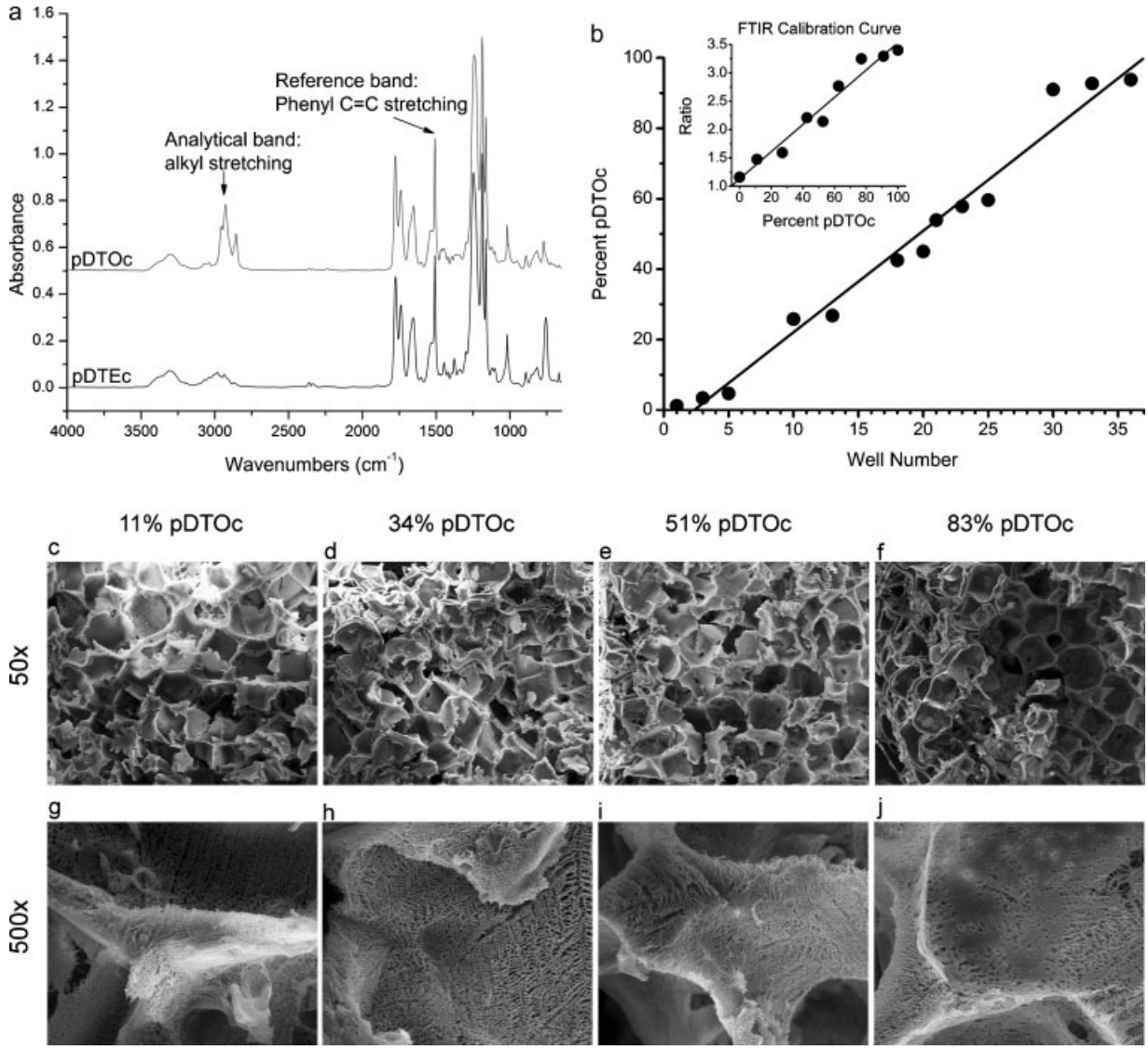

Figure 2. FTIR and SEM measurements for the assessment of the pDTEc/pDTOc scaffold library composition and structural morphology, respectively. a) FTIR spectra of pDTEc and pDTOc after baseline deduction and normalization to maximum absorbance. The spectra were shifted to avoid overlap. For quantification, absorbance at 1508 cm^{-1} was chosen as the reference band, while absorbance at 3000 cm^{-1} was chosen as the analytical band. b) The composition of 13 wells from one library was plotted against the well number. The composition was determined from the peak area ratios (3000 cm^{-1}/1508 cm^{-1}) using a calibration curve (inset) that was made with nine blends of known pDTEc/pDTOc compositions. Lines were fit by linear regression; the Pearson correlation coefficients for the calibration curve (inset) and scaffold libraries (main plot) are 0.98 (t-test; $n = 9$ compositions; $p < 0.001$) and 0.99 (t-test; $n = 13$ compositions; $p < 0.001$), respectively. c–j) SEM images of scaffold cross-sections: scale bars are 500 μm in c–f and 50 μm in g–j. c,g) Well #6 (11% pDTOc); d,h) Well #14 (34% pDTOc); e,i) Well #20 (51% pDTOc); f,j) Well #31 (83% pDTOc). Fifteen scaffolds from one library were imaged for the SEM experiments; representative images are shown.

where voids in the scaffold wall resulting from dioxane sublimation cause 14% porosity and pores from NaCl leaching cause 83% porosity.

Osteoblast adhesion after one day culture in a medium with serum (MWS) appeared uniform across the libraries as measured by the Wst-1 colorimetric cell-viability assay. However, the slope of the line fit to these data by linear regression was significant as determined by a t-test ($p = 0.004$), indicating that cell adhesion was enhanced with increasing pDTEc content in the scaffolds (Fig. 3a). Cell numbers at four days in MWS were higher than at one day in MWS, indicating that cells had proliferated. In addition, osteoblast numbers after four days culture in MWS were enhanced as the pDTEc content increased. A linear regression fit to these data had a significant slope by t-test ($p < 0.001$). Osteoblast adhesion to scaffolds after one day in a serum-free medium (SFM) also

ADVANCED MATERIALS

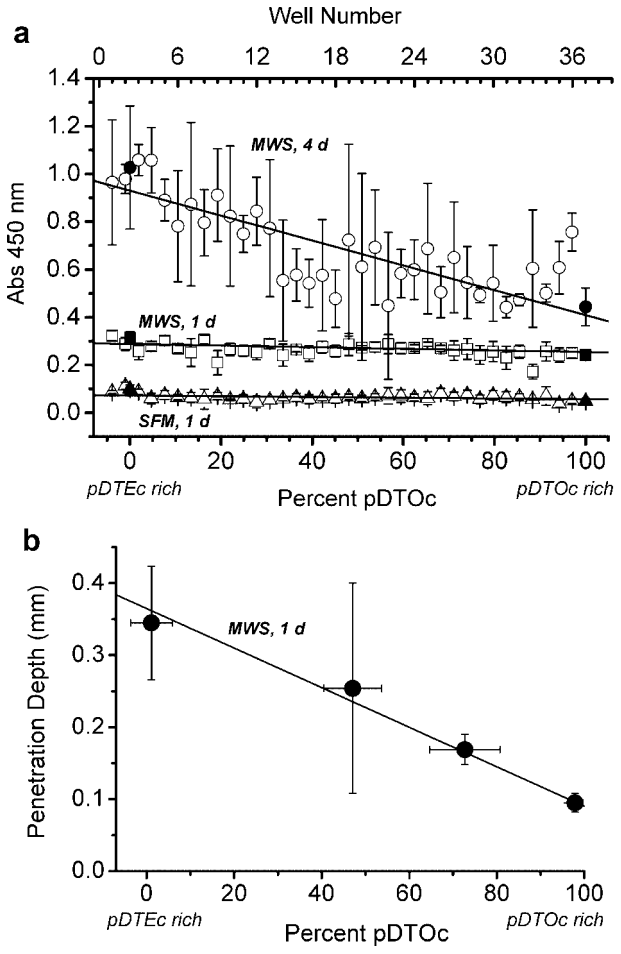

Figure 3. a) Wst-1 assay of MC3T3-E1 cells cultured on scaffold libraries after one day in SFM (open triangles), one day in MWS (open squares), or four days in MWS (open circles). Absorbance at 450 nm is plotted against the scaffold composition on the bottom x-axis and against the well number on the top x-axis. Values for control scaffolds of pure pDTEc and pure pDTOc are given at the end of all three plots using closed triangles (SFM-1d), closed squares (MWS-1d), or closed circles (MWS-4d). Error bars are SD with $n = 3$ libraries. Lines were fit by linear regression ($R = 0.33$ for SFM-1d; $R = 0.44$ for MWS-1d; $R = 0.84$ for MWS-4d) and the slopes for all three plots were significant (t-test; $n = 36$ compositions per plot; $p = 0.004$ for MWS-1d; $p = 0.49$ for SFM-1d; $p < 0.001$ for MWS-4d). Notes: i) two data points for both the one-day and four-days data on the left of the plot go past zero and into negative percent pDTOc due to minor errors in the composition determination by FTIR; ii) the SD is the same as the "combined standard uncertainty of the mean" for the purposes of this work. b) The depth of cell penetration into the library scaffolds after one day in MWS was evaluated using confocal microscopy. Scaffolds from four different regions in one library were evaluated and represent the four data points in the plot. The number of scaffold image stacks (n) analyzed for each data point in the plot going from left to right was 7, 7, 4 and 3, respectively. The line was fit by linear regression ($R = 0.99$).

appeared constant across the libraries (Fig. 3a). The slope of the line fit to these data was significant (t-test; $p = 0.049$) indicating that cell adhesion was also enhanced with increasing scaffold pDTEc content, even in the absence of adsorbed serum proteins. However, the level of significance for one day adhesion in SFM was 12 times lower than that for one day in MWS ($0.049/0.004 = 12$). These results suggest that the protein adsorption plays a role in the observed effect of scaffold composition on cell adhesion.

Evaluation of "within-plate" and "between-plate" repeatability can be used to assess the reproducibility of the combinatorial scaffold-library approach. Each plate contained six control scaffolds each of pure pDTEc and pure pDTOc, which enabled an analysis of the within-plate well-to-well variability for the Wst-1 assay. The average standard deviation (SD) for these sets of six repeats in the same plate was 20% (SD 10%). Next, the between-plate repeatability can be determined since three libraries were used for each of the three treatments (MWS-1d, MWS-4d, SFM-1d). Thus, the average SD for the three wells of the same composition from the three different plates for each of the three treatments was 22% (SD 15%). These SDs compare favorably with the SD of 18% observed for Wst-1 experiments performed on flat substrates.[29] These results indicated that the repeatability of the Wst-1 assay is minimally affected by the scaffold-library format.

Cell morphology was examined by fluorescence confocal microscopy (Fig. 4). More cells were present and cells were better spread on scaffolds rich in pDTEc after one day culture in MWS (Fig. 4a,c,e). After four days in MWS, cells were still more spread in pDTEc-rich scaffolds than in pDTOc-rich scaffolds (Fig. 4g,h). Cells reached confluence on approximately two thirds of the scaffolds (0% to 65% pDTOc), but were sub-confluent on the most pDTOc-rich scaffolds (>65% pDTOc) (not shown). Cells cultured one day in SFM were not well spread and lacked actin filaments (Fig. 4b,d,f). These results suggested that protein adsorption was required for cells to attain a spread morphology on pDTEc-pDTOc scaffolds.

Cell penetration into library scaffolds after one day in MWS was examined by rotating confocal-image stacks and determining the cell penetration-depth (Fig. 3b). Typical penetration depths were 0.1 to 0.3 mm but in many cases cells penetrated more than 0.4 mm into library scaffolds, indicating that cells accessed the 3D environment of the library scaffolds. In addition, cells penetrated further into scaffolds as the pDTEc content increased. Taken together, the Wst-1 and microscopy results indicate that cell adhesion, spreading, proliferation, and penetration into scaffolds were negatively influenced by increasing pDTOc content in the scaffolds. These results also demonstrate how the 3D combinatorial polymer scaffold-library platform can be used to screen for scaffold compositions that promote cell adhesion and proliferation.

The different chemical and physical properties of pDTEc and pDTOc (different side chains, surface energy, glass transition temperatures, mechanical properties, and degradation rate)[21,22] may contribute to the differences in cell response observed in the scaffold libraries. These differences in material properties can also affect the adsorption of serum proteins to the materials, which can contribute to the observed differences in cell response.[30,31] The amount, composition and conformation of serum proteins that adsorb to a surface are

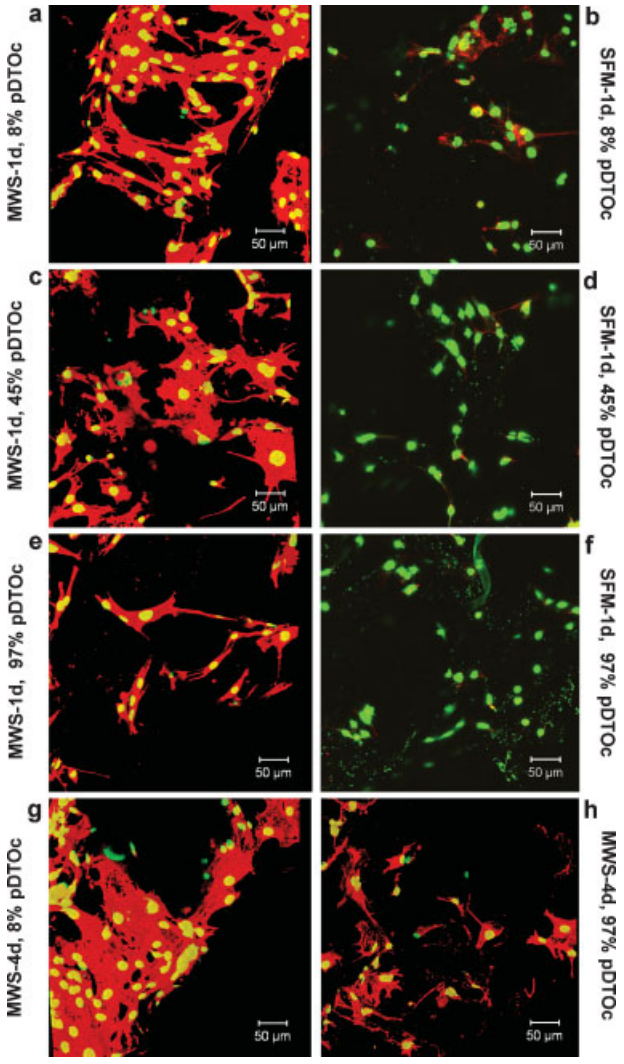

Figure 4. Projection images from confocal microscopy of MC3T3-E1 cells cultured on scaffold libraries after one day (a–f) and four days (g,h) culture in either MWS (a,c,e,g,h) or SFM (b,d,f). A total of three libraries was used for confocal microscopy. One library was used for each of the three treatments (MWS-1d, MWS-4d, SFM-1d) and ten scaffolds were imaged from each of the three libraries. Actin was stained red and nuclei were stained green (but appeared yellow when overlapping with actin). a,b,g) Well #5 (8% pDTOc); c,d) Well #18 (45% pDTOc); e,f,h) Well #36 (97% pDTOc).

strongly influenced by the physical and chemical properties of the substrate.[32] There was a significant trend of increasing cell adhesion with increasing pDTEc content after one day of cell culture in the libraries, both in the presence and absence of serum (Fig. 3a). These results indicate that the pDTEc-pDTOc material properties were influencing cell response. However, the large difference in the significance of the trends ($p = 0.004$ for MWS and $p = 0.049$ for SFM) between MWS and SFM (Fig. 3a) indicates that protein adsorption is also playing a role in determining cell response in the pDTEc-pDTOc scaffold libraries.

Our observations that cell adhesion, spreading, and proliferation were enhanced on pDTEc-rich 3D scaffolds agree with our previous work using 2D films of pDTEc and pDTOc, where cell adhesion, spreading, and proliferation were increased on pDTEc films compared to pDTOc films.[21,22] Our previous results with 2D films[21,22] were predictive of the trend that we have observed with 3D scaffolds. Although studies in other systems have done comparative testing of the same material in 2D and 3D (collagen,[17,20] agarose,[16] and polyurethane[19]), the current work represents a unique data set where two materials (pDTEc and pDTOc) have been tested side by side in both 2D and 3D. These results suggest that relative trends for 3D cell adhesion and proliferation on different materials can be effectively determined using a 2D film format. Further work is required to determine if this will hold true for other cell–material systems.

Fabrication of the scaffold libraries in 96-well plates made assay preparation and analysis very convenient and rapid, because multiprobe tools can be used for liquid transfer and a microplate reader can be used to read absorbance. In addition, the libraries enabled screening of scaffolds of 36 different compositions on each 96-well plate. Moreover, the 96-well libraries could be used for a variety of cell colorimetric assays, such as alkaline phosphatase or enzyme-linked immunosorbent assay (ELISA) kits.

There are both advantages and disadvantages to the currently described 96-well combinatorial scaffold-library approach. Some advantages are that the 96-well arrays are easy to characterize and are amenable to quantitative, high-throughput analyses of cell function such as the colorimetric Wst-1 assay used herein (Fig. 3). However, each well only holds 0.2 mL of medium, which may not be enough for the long-term, high-density cell culture required for mature tissue generation (>14 days). In addition, the scaffolds' bottom and side walls are in close contact with the plate wells. The medium can only access the scaffolds via their top surface; this hinders nutrient/waste exchange and tissue formation deeper in the scaffold. Nevertheless, the 96-well combinatorial-library platform is ideal for screening the effect of scaffold composition and properties on early-stage cell functions such as adhesion and proliferation.

A total of 14 combinatorial scaffold libraries each containing 36 different compositions plus 12 controls (672 individual scaffolds) were prepared for this study (1 for SEM, 1 for FTIR and 12 for cell culture). Scaffolds were fabricated, freeze-dried, salt-leached and used in cell culture tests, all in the same plate. Cell culture work plus SEM and FTIR characterization were completed in six days (not including down-time for salt-leaching, cell incubation, etc.). This compares extremely favorably with the much larger work load, estimated at 24 days, required to conduct the same study using a traditional experimental design where 672 scaffolds of various compositions would be prepared and tested individually. The combinatorial scaffold-library approach is easy to implement and does not require expensive equipment. The approach is also versatile and could be used to test cell responses to a wide range of scaffold properties, such as surface chemistry, surface energy,

ADVANCED MATERIALS

nanoparticles, peptide ligands, pore size, surface topology, or mechanical properties. Finally, the libraries may be adapted to tests beyond those that measure cell responses, such as screening the effect of composition on the scaffold's mechanical properties or degradation behavior.

In summary, we have developed a platform technology for fabricating combinatorial polymer scaffold libraries in a discrete 96-well array format. We demonstrated the feasibility and efficiency of this approach by making libraries of scaffolds with varying compositions of two biodegradable tyrosine-derived polycarbonates, which have different physicochemical properties, pDTEc and pDTOc. Cell screening with osteoblasts showed how the libraries can be used to rapidly identify scaffold formulations that can either promote or suppress cell adhesion and proliferation. To our knowledge, the current work is the first demonstration of a method for fabricating combinatorial library arrays of large-pore scaffolds ($d > 0.1$ mm) that enables screening of cell–material interactions in a 3D format. In conclusion, the three-dimensional scaffold screening platform that we have developed provides a method to accelerate development of novel biomaterials for tissue engineering applications.

Experimental

Fabrication of Combinatorial Scaffold Libraries: Combinatorial scaffold libraries of two tyrosine-derived polycarbonates were fabricated using a novel syringe-pump system (Fig. 1c) [26]. The polymers, pDTEc and pDTOc (weight-average molecular mass 183 000 g/mol and 122 800 g/mol, respectively), were synthesized as described previously [22]. For library fabrication, the two polymer solutions (10% mass/volume in dioxane) were placed in opposing syringe pumps, brought together at a T-junction and mixed in a static mixer. The pumps were programmed so that the effluent from the static mixer changed from pDTEc-rich to pDTOc-rich over time. The effluent from the mixer was deposited into a polypropylene, flat-bottom, 96-well plate (Greiner Bio-One, Monroe, NC) containing 120 mg of sieved NaCl (250 to 425 μm in diameter) per well. Two drops of polymer solution were deposited in each well. Six control scaffolds of pure pDTEc and pure pDTOc were also included in each library. After the deposition, libraries were frozen in liquid nitrogen, freeze-dried overnight to remove solvent, and leached in water for four days to remove NaCl. Libraries were stored in a desiccator until use. An example of a scaffold library is shown in Figure 1d. Well numbers from 1 to 36 were labeled in accordance with the order of deposition. All libraries used in this manuscript were exactly the same as that shown in Figure 1d. Each library had 48 scaffolds: (6 pDTEc controls) + (6 pDTOc controls) + (36 of varied composition). A total of 14 libraries were used for this manuscript: one for SEM, one for FTIR, and 12 for cell culture. For cell culture, three libraries were used for Wst-1 and one library was used for microscopy for each of the three treatments: MWS-1d, MWS-4d and SFM-1d.

FTIR Composition Determination: Composition of the combinatorial polymer scaffold libraries was characterized using FTIR (NEXUS 670 FTIR spectrophotometer, Nicolet, Thermo Electron, Madison, WI). Scaffolds were dissolved in chloroform, cast onto a KBr pellet, and spectra recorded (resolution of 4 cm^{-1}, 64 scans, total range: 650–4000 cm^{-1}). Analysis was performed with OMNIC (Version 7.2, Thermo Electron). A calibration curve was established using FTIR spectra of nine blends of known pDTE-pDTOc composition (Fig. 2b inset). Absorbance at 1508 cm^{-1} was chosen as the reference band (phenyl ring (C=C) stretching), while absorbance at 3000 cm^{-1} was chosen as the analytical band (alkyl stretching) [22]. Peak area ratios of scaffolds (3000 cm^{-1}/1508 cm^{-1}) from the combinatorial scaffold libraries were determined and corresponding compositions were calculated using the calibration curve [25]. Thirteen scaffolds from one library were used for FTIR characterization (Fig. 2b).

Scanning Electron Microscopy: Scaffolds were removed from the 96-well plate, frozen in liquid nitrogen and sectioned with a razor. After sputter-coating with gold, porous structures were viewed by SEM (15 kV, Hitachi S-4700-II FE-SEM, Pleasanton, CA). Fifteen scaffolds from one library were used for SEM characterization.

Cell Culture: The MC3T3-E1 murine osteoblast cell line (Riken Cell Bank, Hirosaka, Japan) was used as a model for osteoblasts [24] and cultured as described [11]. Cultures at low passage (≤6) and 80% confluency were used. Scaffold libraries were sterilized by ethylene oxide and stored for two days in a desiccator under vacuum to degas. Following trypsinization, 10 000 MC3T3-E1 cells in 0.2 mL of medium were seeded onto each scaffold. A total of 12 libraries were seeded with cells using three different treatments as follows: 1) four libraries were seeded with cells in medium with serum (MWS) (α-modification of Eagle's minimum essential medium (Cambrex Bio Science, Walkersville, MD) supplemented with 10% volume fraction fetal bovine serum (Gibco, Rockville, MD) and 0.6% volume fraction kanamycin sulfate (Sigma, Inc., St. Louis, MO)) and incubated for one day; 2) four libraries were seeded in MWS and incubated for four days; 3) four libraries were seeded in serum-free medium (SFM) (same as MWS but without serum) and incubated for one day. Of the four libraries prepared for each of the three treatments (MWS-1d, MWS-4d & SFM-1d), three libraries were analyzed by the Wst-1 assay and one library was used for fluorescence microscopy (described below).

Wst-1 Assay: Cell viability and proliferation on the pDTEc/pDTOc scaffold libraries was assessed using the Wst-1 colorimetric assay for determining cellular dehydrogenase activity (Dojindo, Gaithersburg, MD). [33] Wells were rinsed and incubated for 4 h at 37 °C with 0.2 mL Wst-1 solution; the Tyrode's-Hepes buffer contained 45 μmol/L of Wst-1 [2-(4-iodophenyl)-3-(4-nitrophenyl)-5-(2,4-disulfophenyl)-2H-tetrazolium, monosodium salt] and 2 μmol/L of 1-methoxy-5-methylphenazinium methylsulfate (Dojindo, Gaithersburg, MD). A 0.15 mL aliquot of the Wst-1 reactant was transferred from each well to a new polystyrene 96-well plate and absorbance at 450 nm was measured by a microplate reader (SpectraMax M5, Molecular Devices, Sunnyvale, CA).

Fluorescence Imaging: Cells were fixed (4% volume fraction paraformaldehyde), permeabilized (0.5% volume fraction Triton X-100), and blocked (1% mass fraction bovine serum albumin). Cells were fluorescently stained in phosphate buffered saline (PBS) containing 5 μmol/L Sytox green and 0.2 μmol/L Alexa Fluor 546 phalloidin (both from Invitrogen, Carlsbad, CA). Cells were visualized by a confocal laser scanning microscope (LSM 510, Carl Zeiss, Oberkochen, Germany) equipped with Argon (488 nm) and HeNe (543 nm) lasers. Emission at 560 nm was used to view F-actin filaments stained red by phalloidin while emission at 505–550 nm was used for visualizing nuclei stained by Sytox green. Two objectives, Epiplan-Neofluar 5×/0.15 and Epiplan-Neofluar 20×/0.15, were used. Fifty-slice Z-stacks were collected at 20 and 1.6 μm intervals for the 5× and 20× objectives, respectively. Scaffolds were removed from 96-well plates and observed on slides while moist with PBS.

Cell Penetration Depth: Image stacks collected with the 5× objective (50 slices, 20 μm depth intervals) were used to determine cell penetration-depth into scaffolds after one day culture in MWS (Fig. 3b). Nineteen scaffolds from one library were analyzed. A z-stack was collected from each scaffold and made into a side-view projection image so that the cell penetration-depth could be visualized. The maximum cell penetration-depth at five evenly spaced positions across each side-view projection image was determined and averaged for each scaffold. The yield from this analysis was an average maximum cell penetration-depth for each scaffold analyzed. The penetration-depth

values for these 19 scaffolds were binned into four groups based on composition, averaged and plotted (Fig. 3b).

Received: August 19, 2007
Revised: March 10, 2008
Published online: April 22, 2008

[1] M. J. Lysaght, A. L. Hazlehurst, *Tiss. Eng.* **2004**, *10*, 309.
[2] C. T. Dooley, N. N. Chung, B. C. Wilkes, P. W. Schiller, J. M. Bidlack, G. W. Pasternak, R. A. Houghten, *Science* **1994**, *266*, 2019.
[3] S. P. Rohrer, E. T. Birzini, R. T. Mosley, S. C. Berk, S. M. Hutchins, D.-M. Shen, Y. Xiong, E. C. Hayes, R. M. Parmar, F. Foor, S. W. Mitra, S. J. Degrado, M. Shu, J. M. Klopp, S.-J. Cai, A. Blake, W. W. S. Chan, A. Pasternak, L. Yang, A. A. Patchett, R. G. Smith, K. T. Chapman, J. M. Schaeffer, *Science* **1998**, *282*, 737.
[4] S. Brocchini, K. James, V. Tangpasuthadol, J. Kohn, *J. Biomed. Mater. Res.* **1998**, *42*, 66.
[5] J. C. Meredith, J.-L. Sormana, B. G. Keselowsky, A. J. Garcia, A. Tona, A. Karim, E. J. Amis, *J. Biomed. Mater. Res.* **2003**, *66A*, 483.
[6] D. G. Anderson, S. Levenberg, R. Langer, *Nature Biotech.* **2004**, *22*, 863.
[7] M. D. Disney, P. H. Seeberger, *Chem. Biol.* **2004**, *11*, 1701.
[8] J. R. Smith, A. Seyda, N. Weber, D. Knight, S. Abramson, J. Kohn, *Macromol. Rapid Comm.* **2004**, *25*, 127.
[9] D. G. Anderson, D. Putnam, E. B. Lavik, T. A. Mahmood, R. Langer, *Biomaterials* **2005**, *26*, 4892.
[10] C. J. Flaim, S. Chien, S. N. Bhatia, *Nature Methods* **2005**, *2*, 119.
[11] C. G. Simon, Jr., N. Eidelman, S. B. Kennedy, A. Sehgal, C. A. Khatri, N. R. Washburn, *Biomaterials* **2005**, *26*, 6906.
[12] C. A. Tweedie, D. G. Anderson, R. Langer, K. J. Van Vliet, *Adv. Mater.* **2005**, *17*, 2599.
[13] D. G. Anderson, C. A. Tweedie, N. Hossain, S. M. Navarro, D. M. Brey, K. J. Van Vliet, R. Langer, J. A. Burdick, *Adv. Mater.* **2006**, *18*, 2614.
[14] A. J. Urquhart, D. G. Anderson, M. Taylor, M. R. Alexander, R. Langer, M. C. Davies, *Adv. Mater.* **2007**, *19*, 2486.
[15] L. D. Shea, D. Wang, R. T. Franceschi, D. J. Mooney, *Tiss. Eng.* **2000**, *6*, 605.
[16] P. D. Benya, J. D. Shaffer, *Cell* **1982**, *30*, 215.
[17] H. G. Hall, D. A. Farson, M. J. Bissell, *Proc. Natl. Acad. Sci* **1982**, *69*, 4672.
[18] A. Abbott, *Nature* **2003**, *424*, 870.
[19] K. Webb, W. Li, R. W. Hitchcock, R. M. Smeal, S. D. Gray, P. A. Tresco, *Biomaterials* **2003**, *24*, 4681.
[20] L. Meinel, V. Karageorgiou, R. Fajardo, B. Snyder, V. Shinde-Patil, L. Zichner, D. Kaplan, R. Langer, G. Vunjak-Novakovic, *Ann. Biomed. Engin.* **2004**, *32*, 112.
[21] L. O. Bailey, M. L. Becker, J. S. Stephens, N. D. Gallant, C. M. Mahoney, N. R. Washburn, A. Rege, J. Kohn, E. J. Amis, *J. Biomed. Mater. Res.* **2006**, *76*, 491.
[22] S. I. Ertel, J. Kohn, *J. Biomed. Mater. Res.* **1994**, *28*, 919.
[23] J. Kohn, *Med. Device Develop.* **2006**, *1*, 35.
[24] H. Sudo, H. A. Kodama, Y. Amagai, S. Yamamoto, S. Kasai, *J. Cell Biol.* **1983**, *96*, 191.
[25] N. Eidelman, C. G. Simon, *J. Res. Natl. Inst. Stan.* **2004**, *109*, 219.
[26] C. G. Simon, Jr., J. S. Stephens, M. L. Becker, *Rev. Sci. Instrum.* **2007**, *78*, 072207-1.
[27] J. J. Klawitter, S. F. Hulbert, *J. Biomed. Mater. Res.* **1971**, *2*, 161.
[28] E. Tsuruga, H. Takita, H. Itoh, Y. Wakisaka, Y. Kuboki, *J. Biochem.* **1997**, *121*, 317.
[29] C. G. Simon, Jr., C. A. Khatri, S. A. Wight, F. W. Wang, *J. Orthopaed. Res.* **2002**, *20*, 473.
[30] N. Weber, D. Bolikal, S. L. Bourke, J. Kohn, *J. Biomed. Mater. Res.* **2004**, *68A*, 496.
[31] N. Weber, H. P. Wendel, J. Kohn, *J. Biomed. Mater. Res.* **2005**, *72A*, 420.
[32] T. A. Horbett, in *Biomaterials: Interfacial Phenomena and Applications*, (Eds: S.L. Cooper, N. A. Peppas,), ACS, Washington, DC **1982**, p. 233.
[33] M. Ishiyama, M. Shiga, K. Sasamoto, M. Mizoguchi, P. G. He, *Chem. Pharm. Bull.* **2005**, *41*, 1118.

